

AD-A105 224 ARMY ARMAMENT RESEARCH AND DEVELOPMENT COMMAND DOVER--ETC F/G 14/2

CARS SPECTROSCOPY OF GUN PROPELLANT FLAMES.(U)

SEP 81 L E HARRIS, M E MCILWAIN

ARLCD-TR-81007

UNCLASSIFIED

NL

1-1  
OF  
44/224



END  
DATE  
FILMED  
0 81  
DTIC

12

LEVEL II

1

AD

AD-8430 002

AD A105224

TECHNICAL REPORT ARLCD-TR-81007

# CARS SPECTROSCOPY OF GUN PROPELLANT FLAMES

L. E. HARRIS  
M. E. MCILWAIN

DTIC  
ELECTE  
S OCT 7 1981 D  
B

SEPTEMBER 1981



US ARMY ARMAMENT RESEARCH AND DEVELOPMENT COMMAND  
LARGE CALIBER  
WEAPON SYSTEMS LABORATORY  
DOVER, NEW JERSEY

APPROVED FOR PUBLIC RELEASE; DISTRIBUTION UNLIMITED.

FILE COPY

81 10 5 083

The views, opinions, and/or findings contained in this report are those of the author and should not be construed as an official Department of the Army position, policy or decision, unless so designated by other documentation.

Destroy this report when no longer needed. Do not return to the originator.



UNCLASSIFIED

SECURITY CLASSIFICATION OF THIS PAGE(When Data Entered)

20. ABSTRACT (cont)

separated sequence of single pulse CARS spectra indicated turbulent air mixing in these propellant flames. The results demonstrated that temporal and spatially resolved temperature measurements could be determined in transient, turbulent flames.

9

UNCLASSIFIED

SECURITY CLASSIFICATION OF THIS PAGE(When Data Entered)

## CONTENTS

	Page
Introduction	1
Cars Process	1
Experimental	3
Temperature Determination	3
Flame Measurements	4
Discussion	5
References	7
Distribution List	19

## TABLES

1 SGP-38 propellant composition	4
2 Thermochemical calculations	4

## FIGURES

	Page
1 CARS energy level diagram	8
2 Phase matching configuration for gases	9
3 CARS instrumental schematic	10
4 CARS nitrogen spectrum from a premixed propane and air flame taken using a single pulse $I_{\max} = 80$ counts	11
5 Height of the 1-2 band (relative to a 0-1 band normalized to one) with respect to change in temperature	12
6 CARS nitrogen spectrum of premixed propane and air flame obtained by averaging ten pulses	13
7 Variation of temperature with respect to vertical position above the burner surface (mm) in a premixed propane and air flame	14



## INTRODUCTION

Accurate in situ determination of gas and flame temperature and species concentrations are required for elucidating the complex dynamics involved in ballistic events. As new propellant materials are developed, these measurements can provide a means of evaluating their ballistic properties and are useful for comparison with ballistic computer calculations.

A wide data base of experimentally measured propellant flame temperatures and in situ species concentrations is nonexistent primarily because propellant flames are transient, turbulent, particle-laden, and luminous. These properties of propellant flames make conventional measurements, such as line reversal and Raman, difficult or impossible to perform. A relatively new technique [Coherent Anti-Stokes Raman Scattering (CARS)] may greatly facilitate in situ measurements. Recently CARS spectroscopy has been used to investigate not only stationary laboratory flames but also flames of practical interest (refs 1 through 4). The results of these studies indicate that CARS measurements can be performed upon nonideal flames such as those produced by propellants.

## CARS PROCESS

The CARS process (fig. 1) involves the interaction of two high intensity laser beams (pump and Stokes beams) at angular frequencies  $\omega_1$  and  $\omega_s$ . When the phase of the two frequencies is matched and the difference between  $\omega_1$  and  $\omega_s$  is equal to a vibrational frequency of the gas being probed, an anti-Stokes photon is generated at

$$\omega_{as} = 2\omega_l - \omega_s \quad (1)$$

The intensity of the anti-Stokes emission is related to the induced polarization of the medium which is expressed as

$$P(\omega) = \chi^{(1)}E + \chi^{(2)}E^2 + \chi^{(3)}E^3 \quad (2)$$

where  $P$  is the induced polarization,  $\chi$  is the dielectric susceptibility, and  $E$  is the electric field strength. It can be shown that for homogenous media the CARS process is proportional to the third order susceptibility and the power generated at the anti-Stokes frequency is

$$P\omega_{as} = A \left( \frac{\omega_{as}}{\eta_{as}} \right)^2 / 3\chi^{(3)} / 2P\omega_l^2 P\omega_s \quad (3)$$

where  $A$  is a constant,  $\eta$  is the refractive index at  $\omega_{as}$ ,  $P$  is the laser power, and  $/3\chi^{(3)}/$  is the magnitude of the total third order susceptibility. The total third order susceptibility of the medium is composed of frequency dependent (resonant) and independent (non-resonant) terms

$$/3\chi^{(3)}/2 = \chi_R^2 + 2\chi_R \cdot \chi_{NR} + \chi_{NR}^2 \quad (4)$$

For a simple, damped harmonic oscillator  $\chi_R$  is expressed as

$$\chi_R = K \Delta N_i / [2(\omega_{ij} - (\omega_l - \omega_s)) - i\Gamma] \quad (5)$$

where  $\omega_{ij}$  is the ro-vibrational frequency,  $\Gamma$  is the Raman linewidth,  $\Delta N_i$  is the population difference between the upper and lower states for a particular transition, and K is defined as

$$K = \frac{Nc^4}{K\omega_s^4} \left( \frac{d\sigma}{d\Omega} \right) \quad (6)$$

where N is the total number density, c is the speed of light, and  $\frac{d\sigma}{d\Omega}$  is the Raman scattering cross section.

The above expressions assume that all frequencies are phase matched which can be experimentally accomplished in two ways for gaseous molecules. The  $\omega_l$  and  $\omega_s$  beams can be combined on a straight line or at large angular separations called BOXCARS (ref 5). As shown in figure 2, the BOXCARS Phase matching conditions are satisfied by

$$2 n_l \omega_l \cos \alpha = n_s \omega_s \cos \theta + n_{as} \omega_{as} \cos \delta \quad (7)$$

where  $n_l$  is the refractive index at wavelength l.

Although the CARS process is related to conventional Raman scattering, the technique has the following advantages:

1. The light emitted during the CARS process is shifted to higher frequencies than  $\omega_l$ , eliminating laser produced fluorescent interferences.
2. The process of mixing the various laser beams produces coherent (beam-like) emission which can be efficiently captured and detected.
3. The stimulated nature of the process greatly enhances the conversion efficiency of the blue shifted anti-Stokes emission so that it is several orders of magnitude greater in intensity than normal Raman.
4. The mixing geometry of the laser beams produces emission from discrete and easily identified volumes.
5. The pulse nature of the lasers used to generate the CARS process allows for sufficient temporal resolution to freeze out the chemical and fluid dynamics.

These aspects of CARS make the technique attractive for probing transient flames.

The primary purpose of these CARS experiments was to determine the reliability of the CARS technique for making temperature measurements and to demonstrate the feasibility of using the technique to probe transient, turbulent flames.

## EXPERIMENTAL

CARS spectra are generated by use of the apparatus shown in figure 3. The pump laser beam is produced by a Quanta-Ray DCR-1A Nd/YAG laser. The output of the Nd/YAG laser at 1.06 microns (800 mj) is doubled to generate the pump beam at 5320 Å (250 mj) which has a bandwidth less than  $2 \text{ cm}^{-1}$ . The pump beam is separated from the primary beam using prisms. Forty percent of the pump beam is split off ( $BS_1$ ) to pump a dye laser to generate the Stokes beam. The dye laser is operated broadband at 6073 Å (10 mj) with a  $150 \text{ cm}^{-1}$  bandwidth. In BOXCARS configuration the pump beam is split into two components which are spatially separated to form an angle,  $2\alpha$ , when focused. The Stokes beam is introduced at a second angle,  $\theta$ , in the plane of the pump beams so that phase matching occurs. CARS is generated in the region where the three beams cross at a third angle,  $\gamma$ . To achieve BOXCARS geometry, the pump beam is split using a 50 % beamsplitter ( $BS_2$ ). The  $\omega_1$  beam is reflected from a dichroic (DC) which transmits the Stokes beam, and  $\omega_1'$  is separately reflected along another path so that the pump beams are separated at the focusing lens. The BOXCARS signal is generated along  $\omega_1'$  and, after dispersal and spatial separation with an aperture, is focused on the slits of a monochromator fitted with a PAR SIT detector. The signal from the detector is subsequently sent to an OMA2 for processing.

In these experiments a 250 mm focusing lens was used with a pump beam crossing angle of  $5^\circ$ . This configuration has been shown experimentally (ref 5) to give a spectral resolution near  $1 \text{ nm}^3$ . A 1/4 meter monochromator equipped with an 1800 line per/mm grating gave an experimental spectral resolution of  $8.00 \text{ cm}^{-1}$  with  $2.5 \text{ cm}^{-1}$  per channel.

Measurements were made on a premixed propane/air flame maintained on a 1.6-cm-diameter circular burner surface constructed of a matrix of steel syringe needles 0.2 cm outer diameter. The flame was stabilized by flowing  $N_2$  through a 2-cm-diameter concentric outertube. The flow rates of propane and air were adjusted to approximately 130 and 2000  $\text{cm}^3$  per min, respectively.

The propellant used was U.S. Navy SGP-38, which has the composition given in table 1. The propellant samples, in the form of right-circular cylinders 12-mm long, were burned in air.

Shadowgraphs of the propellant flame were produced with an argon spark of approximately 1.0 microsecond duration with a Z-fold optical configuration.

### Temperature Determination

In most air fed flames, nitrogen is a major inert constituent in the burning gases issuing from the burner. An abundance of nitrogen is also predicted in propellant flames by thermochemical calculations (table 2). Nitrogen is a convenient molecule to detect and use as an in situ gas thermometer. The actual process of measuring a nitrogen CARS spectrum does not directly yield the gas temperature. The shape of the spectral profile is indicative of the gas temperature. The change of the spectral profile must be calculated. A computer model

is used to produce synthetic spectra. The input to this program is the gas temperature, the molecular constants of the probe gas, and the value for the nonresonant susceptibility which accounts for the influence of other flame constituents observed in experimental spectra. The scheme used to generate these computer synthesized spectra is described in reference 6. The energy of the vibrational and rotational transitions are calculated and individual level populations are assumed to follow a Boltzman distribution.

These energies and populations are convoluted by equation 3 and the resulting intensities are plotted as a function of  $\omega_1 - \omega_s$ . These synthetic spectra can be compared directly to experimental spectra as displayed in figure 4 or in cases where the hot band [(2-1) band] is present, its height is compared to the curve shown in figure 5 to estimate the gas temperature.

Table 1. SGP-38 propellant composition

<u>Component</u>	<u>Weight %</u>
Nitrocellulose (12%)	47.5
Metriol trinitrate	39.4
Triethyleneglycol dinitrate	10.0
Ethyl centralite	1.0
Lead beta resorilate	1.0
Cryolite	1.0
Cordella wax	1.0

Table 2. Thermochemical calculations

	P = 1 ATM					T = 2600 K				
	<u>CO</u>	<u>CO<sub>2</sub></u>	<u>H<sub>2</sub></u>	<u>H<sub>2</sub>O</u>	<u>N<sub>2</sub></u>					
Mole fraction	0.43	0.07	0.18	0.19	0.10					

#### Flame Measurements

To assess the ability of our computer model to accurately determine flame temperatures, a number of spectral measurements were determined at various positions in a slightly fuel rich propane/air flame. CARS spectra were collected both during a single laser shot and as an average of single shot spectra. Single shot spectra (fig. 4) were obtained, while averaged spectra resembled that displayed in figure 6.

The modeled spectrum (figs. 4 and 6) is in agreement with the average spectra and, considering the low signal to noise for the single shot spectrum, the fit is acceptable.

The gas temperature is displayed in figure 7 as a function of position in the premixed flame. As expected for premixed flames maintained on a flat flame burner, the temperature remains nearly constant across the width and height of the flame. Measured temperatures can be compared to that calculated for a stoichiometric flame (2250 K) and determined for a propane/air diffusion flame (2150 K).

To determine the accuracy of the CARS temperature measurements additional measurements were made using the sodium line reversal technique. The CARS and sodium line reversal temperatures are compared in figure 8. The average difference between temperatures determined by the two methods at the same point in the flame is 30.1 K.

To determine the feasibility for CARS temperature determinations in non-ideal flames, CARS spectra were recorded in propellant flames at various positions along the flame centerline above the burning propellant surface. For simplicity the experiments were carried out in air at atmospheric pressure. The single pulse spectra (fig. 9) were produced at 0.1 second intervals approximately 63 mm above the propellant surface. The dramatic difference in spectral profile and analyzed temperatures were an indication of turbulence and mixing of the hot gases with air. A CARS spectrum was also produced at approximately 10 mm above the surface in a single pulse (fig. 10). Although the spectrum was reduced in intensity and had a much lower signal to noise ratio, it was analyzed to yield a gas temperature.

#### DISCUSSION

The reference flame results confirm the usefulness of CARS spectroscopy for flame temperature determination. The 2050 K maximum temperature measured for the premixed propane/air flame is not unrealistic considering the position above the burner where measurements were made, the stoichiometry of the gases, and the burner design. The average agreement with Na line reversal temperatures is  $\pm 30$  K. This is consistent with other CARS measurements recorded at lower temperatures and those reported in the literature (ref 4), which determined the error for temperatures evaluated in this manner to be  $\pm 50$  K. Using this error the propane/air flame temperatures are consistent with those reported for a propane diffusion flame (ref 4). The similarity between diffusion and premixed flame temperatures is not surprising. It is expected that only the positions of maximum temperature are dependent upon flame type, since the same chemistry must occur in both flame types (ref 7). The agreement with reported flame temperatures, calculated values, and those determined in this work increases the validity of CARS temperature determination.

The initial attempt to use CARS to investigate actual propellant flames was successful. The nitrogen CARS signal intensity was sufficient to obtain flame temperature even for the spectrum recorded near the propellant surface. At this

position one would expect that all nitrogen present was produced by the propellant combustion, since the mass flow from the surface would be sufficient to retard air from diffusing into this region. Typically, the materials produced considerable amounts of soot and incandescence on burning. Yet, the measurements were relatively free from interferences, and the only interference observed was due to large particles blocking one or more beams.

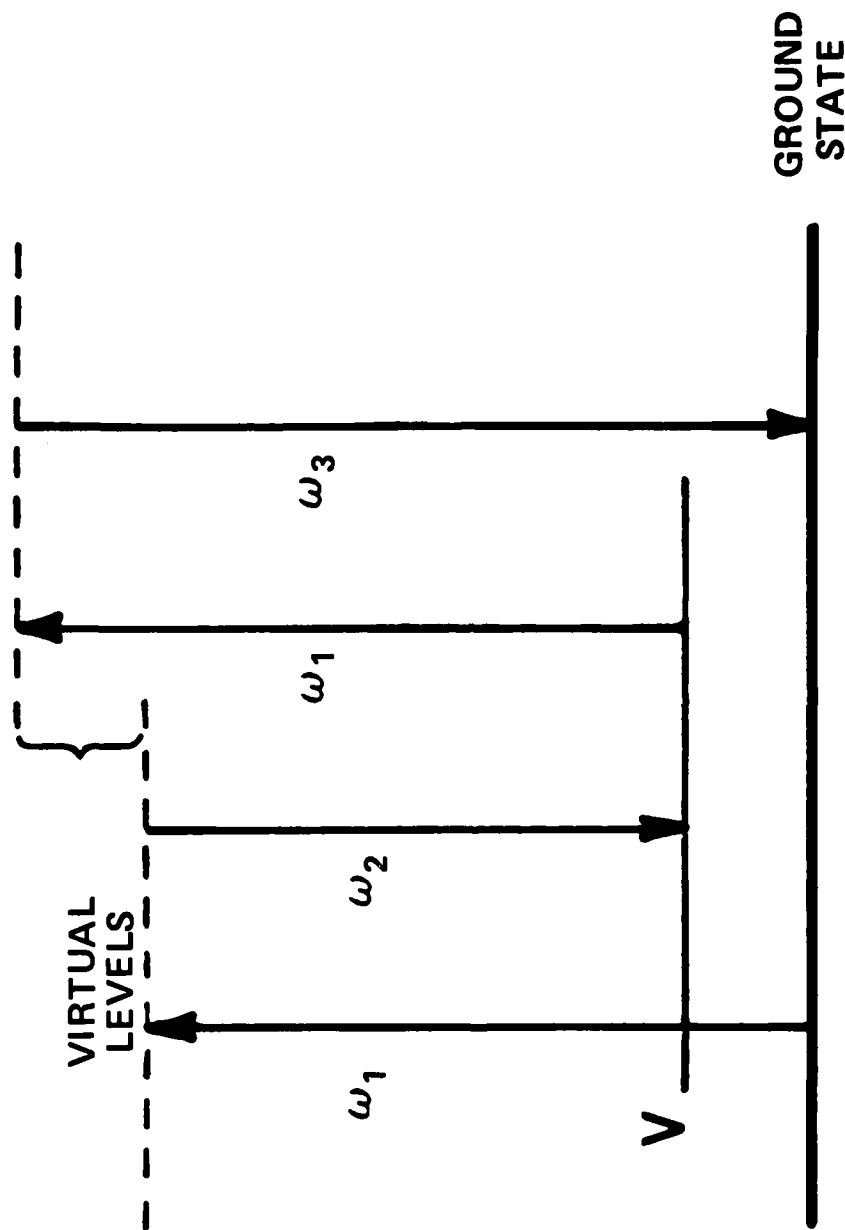
The high temperature measured near the propellant surface, 2500 K, is in satisfactory agreement with the calculated flame temperature of 2600 K. The range of temperature determined from spectra obtained at 63 mm above the propellant surface is indicative of turbulent flow and mixing of surrounding air with hot combustion gases. The mixing process is further substantiated by shadowgraphs such as that shown in figure 11, which display eddies and dark zones at this position in the propellant flame.

The unconfined burning of the propellant in air limits the interpretation of the measured flame temperature in relation to combustion models such as the Parr-Crawford nitrocellulose model, (ref 8). The influence of air on these reaction zones alters the chemical reactions which occur and affect heat feedback to the solid surface. Further work is required to better understand the influence of air in this reaction scheme.

#### REFERENCES

1. S. A. J. Druet and J. P. E. Taran, "Coherent Anti-Stokes Raman Spectroscopy in Chemical and Biological Application of Lasers," C. B. Moore, ed., Academic Press, pp 187-252, 1979.
2. J. W. Nibbler, W. M. Shaub, J. R. McDonald and A. B. Harvey, "Coherent Anti-Stokes Raman Spectroscopy in Vibrational Spectra and Structure," vol 6, J. R. Durig, ed., Elsevier, Amsterdam, pp 173-225, 1977.
3. B. Attal, M. Pealat, and J. E. P. Taran, paper presented at the 1980 Winter meeting of the AIAA.
4. A. C. Eckbreth and R. J. Hall, Combustion and Flame, vol 36, p 87, 1979.
5. A. C. Eckbreth, Appl. Phys. Letter, vol 32, p 47, 1979.
6. R. J. Hall, Combustion and Flame, vol 35, p 47, 1979.
7. B. Lewis and G. von Elbe, Combustion, Flames and Explosives of Gases, Academic Press, Inc., 1961.
8. R. G. Parr and B. C. Crawford, J. Phys. Chem, vol 54, p 929, 1950.

EXCITED  
ELECTRONIC  
STATE

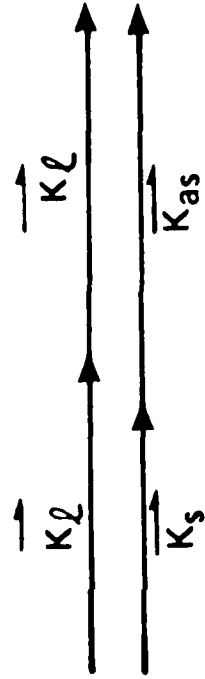


GROUND  
STATE

$\omega_1$ ,  $\omega_2$  and  $\omega_3$  = angular frequencies of the pump,  
 Stokes and CARS beams, respectively

Figure 1. CARS energy level diagram

### COLLINEAR



### BOXCARS

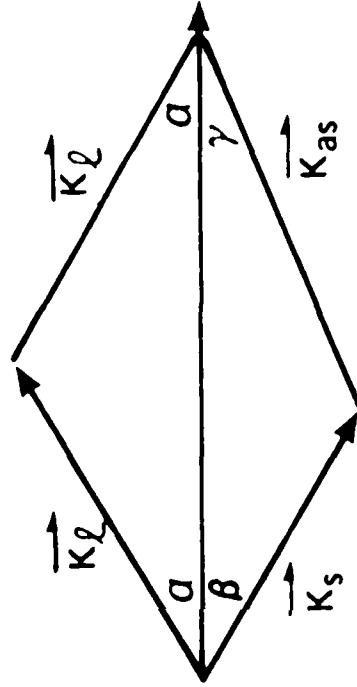


Figure 2. Phase matching configuration for gases

BS = beamsplitter, M = mirror, OF = optical flat,  
 DC = dichroic, T = optical trap,  
 SIT = silicon intensified target detector,  
 OMA = PAR optical multichannel analyser

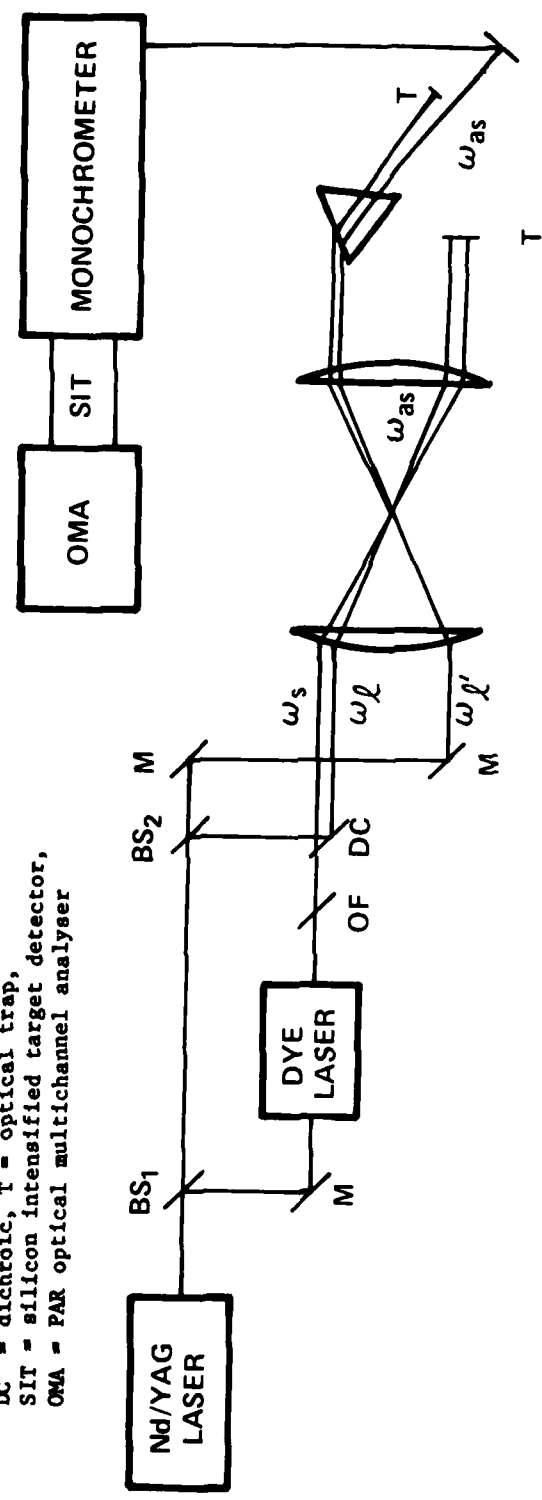


Figure 3. CARS instrumental schematic

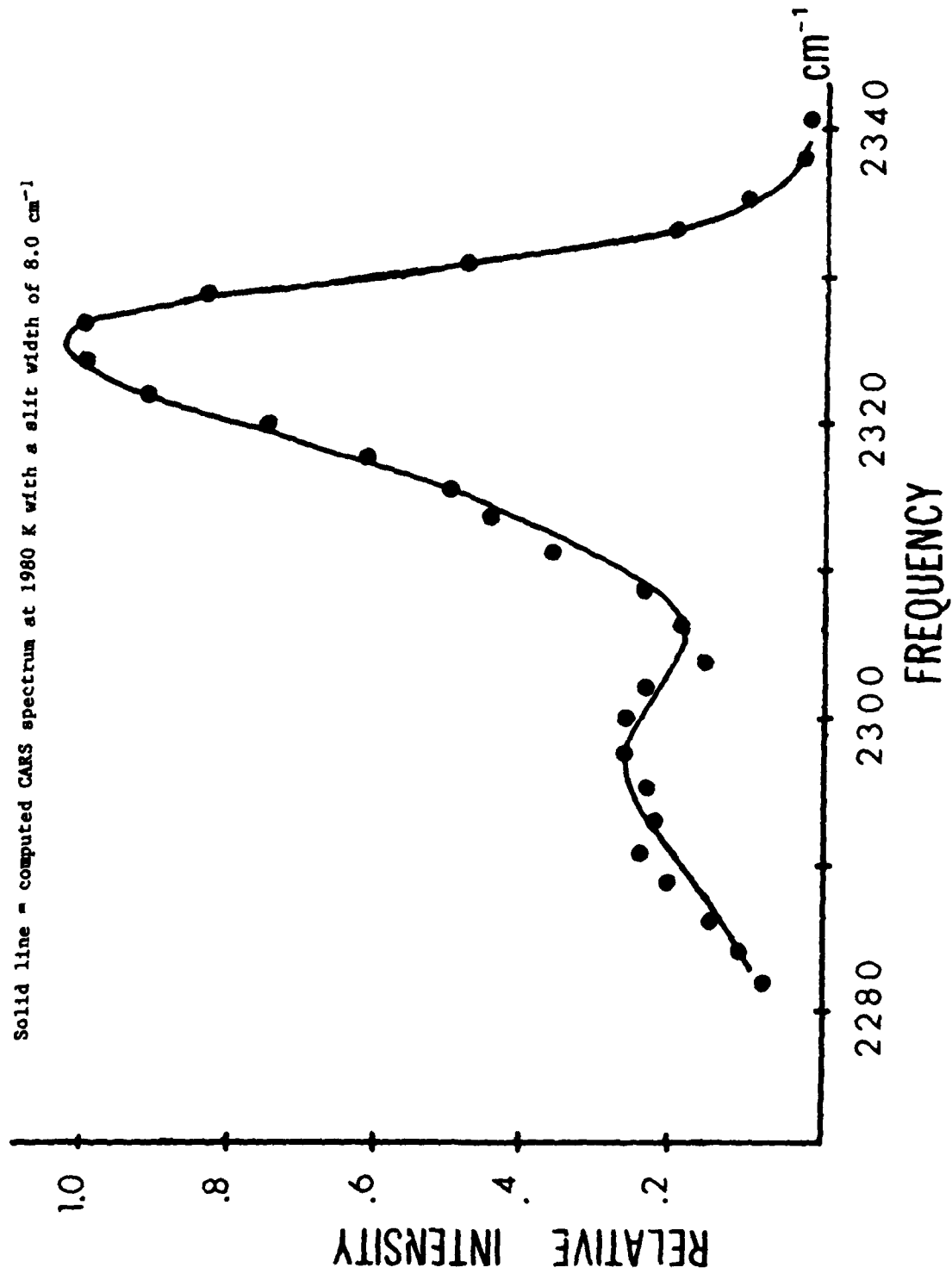


Figure 4. CARS nitrogen spectrum from a premixed propane and air flame taken using a single pulse  $I_{\text{max}} - 80$  counts

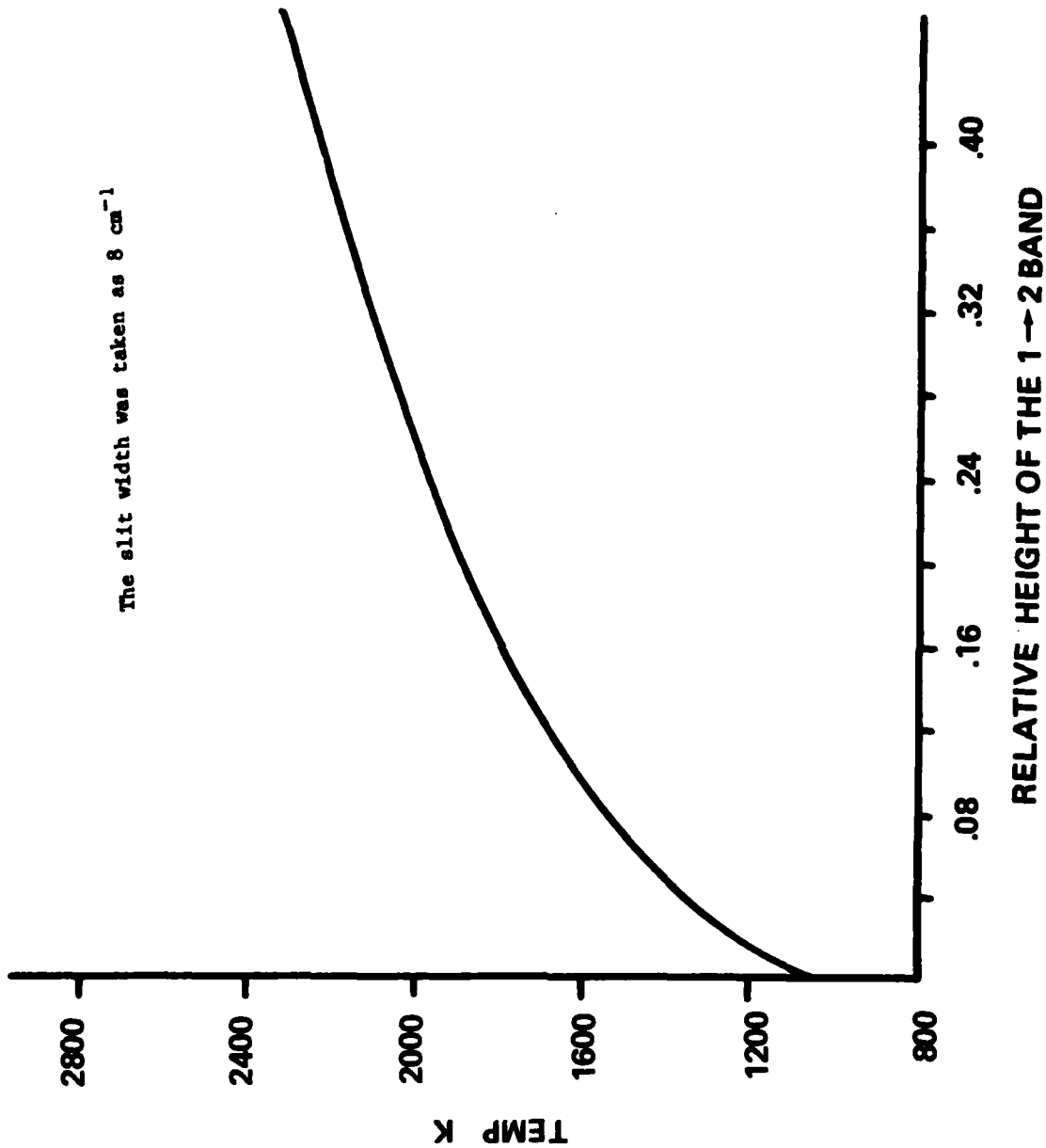


Figure 5. Height of the 1-2 band (relative to a 0-1 band normalized to one) with respect to change in temperature

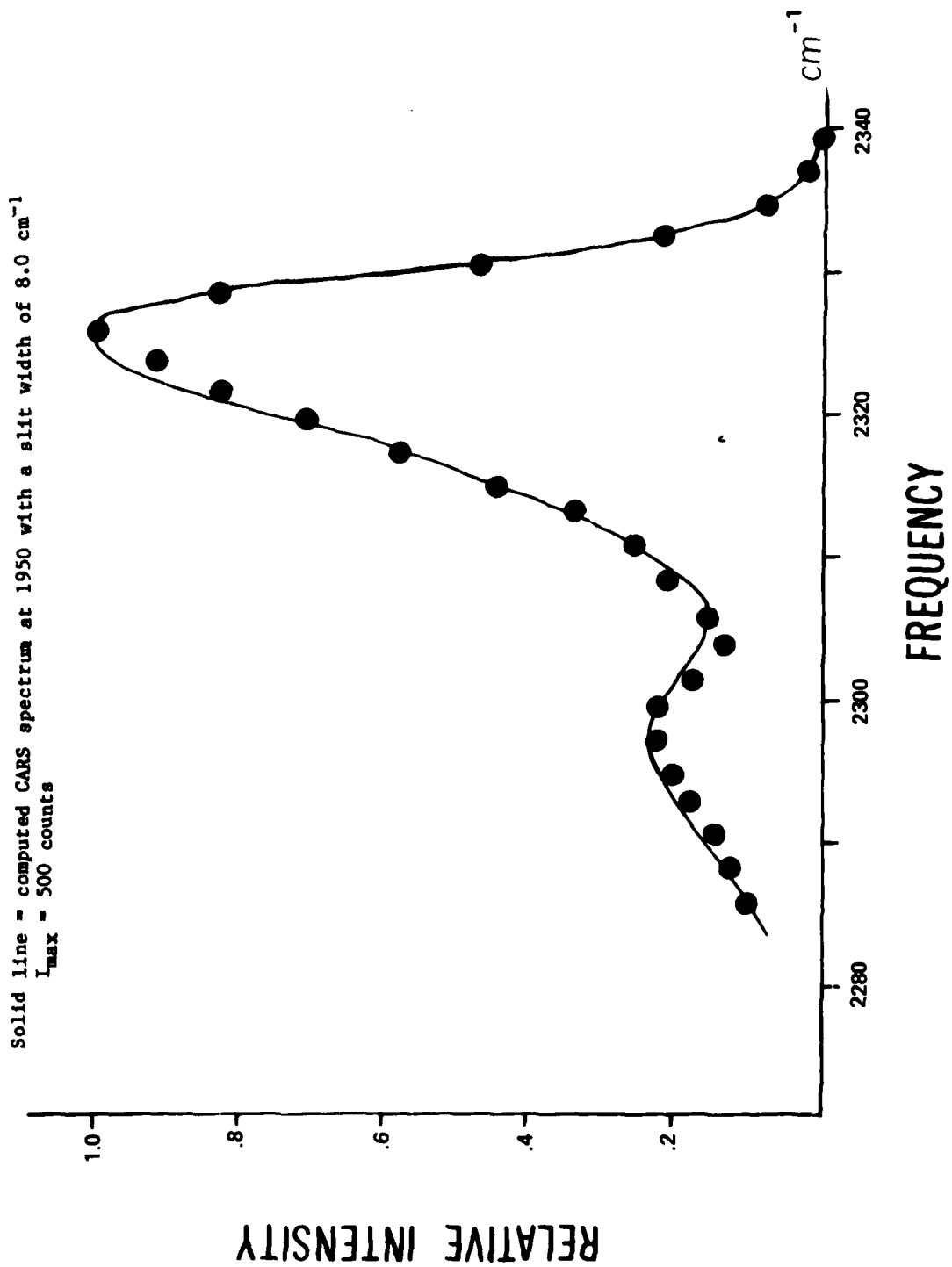


Figure 6. CARS nitrogen spectrum of premixed propane and air flame obtained by averaging ten pulses

Values in parenthesis represent horizontal displacement (mm) from the burner centerline. Burner halfwidth is 8 mm.

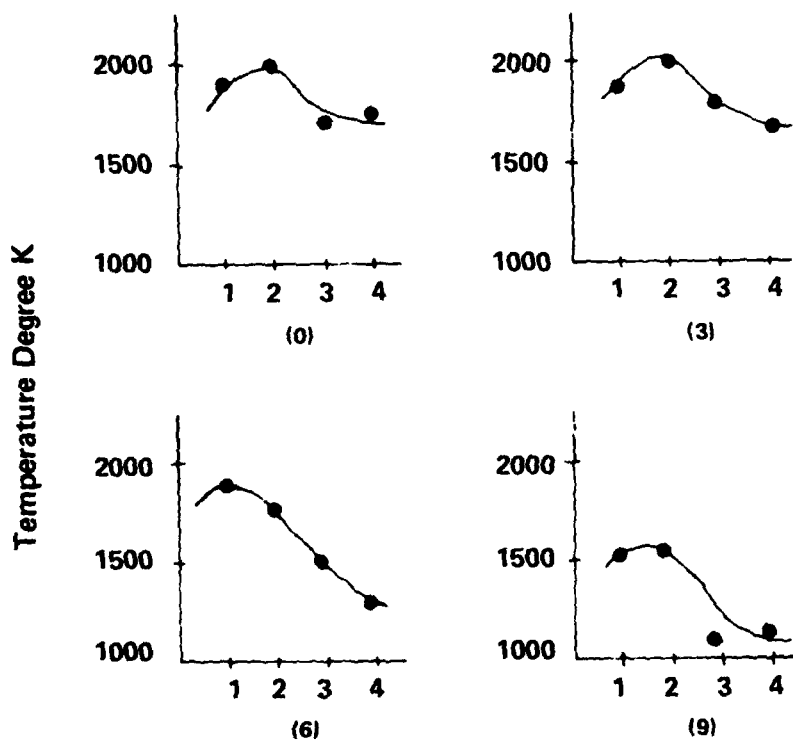
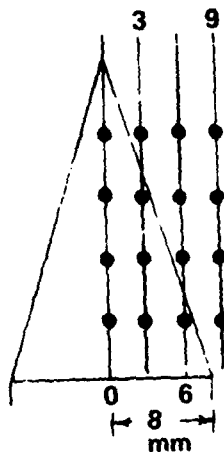


Figure 7. Variation of temperature with respect to vertical position above the burner surface (mm) in a premixed propane and air flame

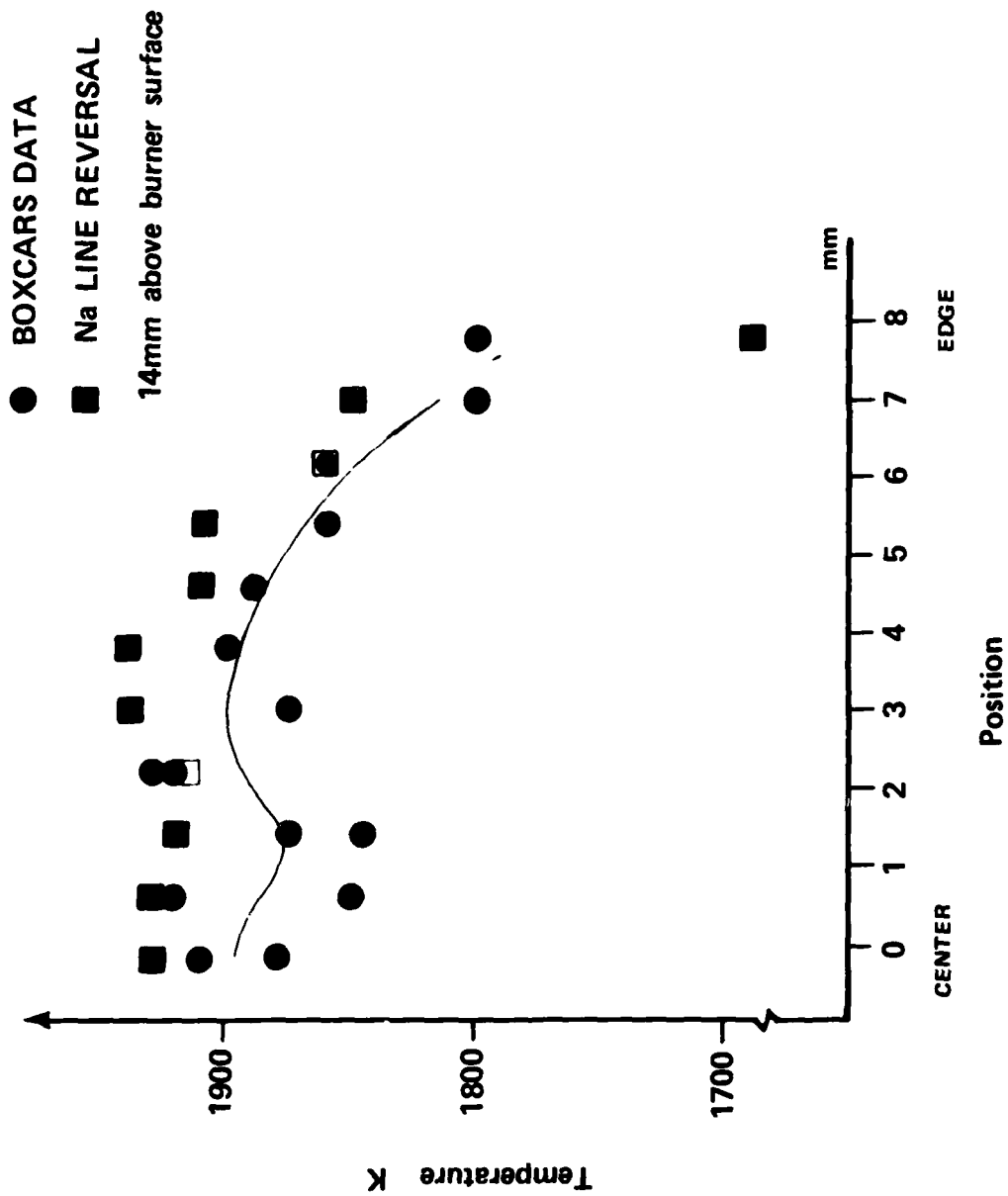


Figure 8. Temperature determined by CARS and Na line reversal in a premixed propane and air flame with respect to horizontal displacement from the burner centerline (mm)

Top spectrum:  $I_{\max} = 1312$  counts,  $T = 2175 \pm 50$  K  
 Middle spectrum:  $I_{\max} = 179$  counts,  $T = 2450 \pm 150$  K  
 Bottom spectrum:  $I_{\max} = 675$  counts,  $T = 1950 \pm 75$  K

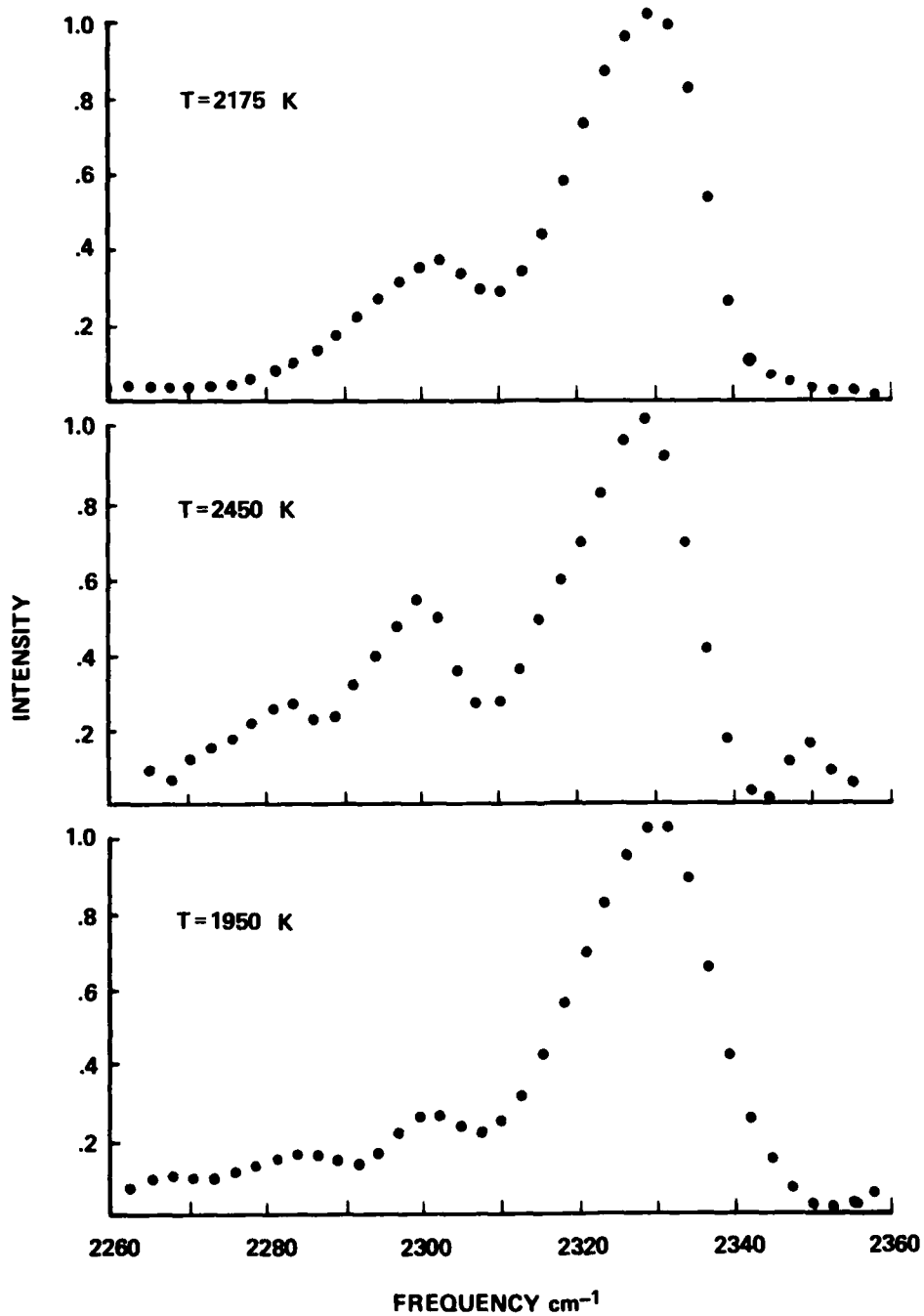
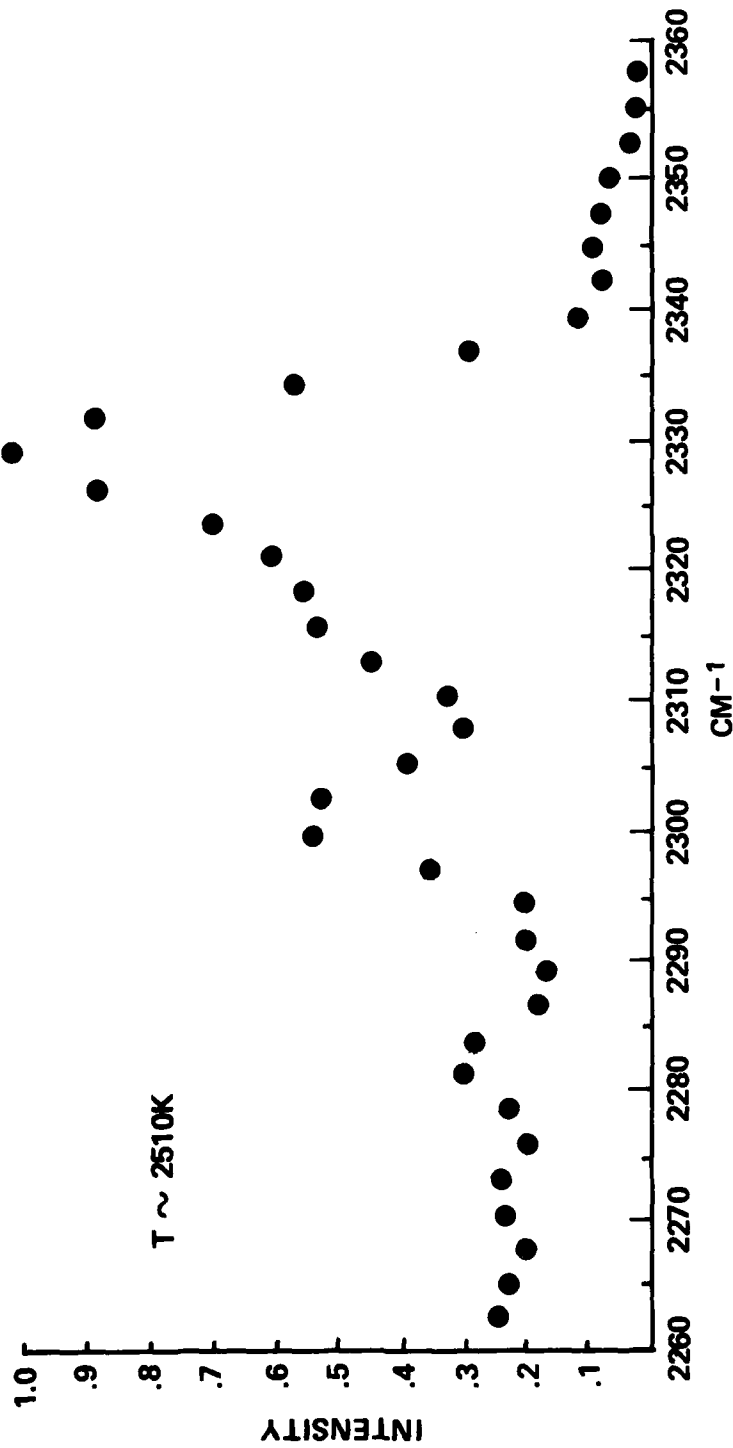


Figure 9. CARS nitrogen spectra of SGP-38 propellant flame burning in air taken using single pulses 0.1 sec apart 63 mm above the centerline of the propellant surface



$I_{\max} = 212$  counts,  $T = 2500 \pm 150$  K

Figure 10. CARS nitrogen spectrum of SGP-38 propellant flame burning in air taken using single pulse 10 mm above the centerline of the propellant surface



Figure 11. Shadowgraph of propellant flame taken using an Argon spark of one microsecond duration

DISTRIBUTION LIST

Commander  
Defense Technical Information Center  
ATTN: Accessions Division (12)  
Cameron Station  
Alexandria, VA 22314

Director  
Defense Advanced Research Projects Agency  
ATTN: LTC C. Buck  
1400 Wilson Boulevard  
Arlington, VA 22209

Director  
Institute for Defense Analyses  
ATTN: H. Wolfhard  
R. T. Oliver  
400 Army-Navy Drive  
Arlington, VA 22202

Commander  
U.S. Army Materiel Development  
and Readiness Command  
ATTN: DRCDMD-ST  
5001 Eisenhower Avenue  
Alexandria, VA 22333

Commander  
U.S. Army Armament Research  
And Development Command  
ATTN: DRDAR-TSS (5)  
DRDAR-GCL  
DRDAR-LC, J. Frasier  
DRDAR-LCA, H. Fair  
DRDAR-LCA-G, D. Downs  
L. Harris  
T. Vladimiroff  
A. Beardell  
J. Lannon  
Y. Carignon  
DRDAR-LCE, R. Walker  
P. Marinkas  
C. Capellos  
F. Owens

Dover, NJ 07801

Commander  
U.S. Army Armament Materiel  
and Readiness Command  
ATTN: DRSAR-LEP-L, Tech Lib  
Rock Island, IL 61299

Director  
Benet Weapons Laboratory  
U.S. Army ARRADCOM  
ATTN: DRDAR-LCB-TL  
Watervliet, NY 12189

Commander  
U.S. Army Watervliet Arsenal  
ATTN: SARWV-RD, R. Thierry  
Watervliet, NY 12189

Commander  
U.S. Army Aviation Research  
and Development Command  
ATTN: DRSAV-E  
P.O. Box 209  
St. Louis, MO 63166

Director  
U.S. Army Air Mobility Research  
and Development Laboratory  
Ames Research Center  
Moffett Field, CA 94035

Commander  
U.S. Army Communications Research  
and Development Command  
ATTN: DRDCO-PPA-SA  
Fort Monmouth, NJ 07703

Commander  
U.S. Army Electronics Research  
and Development Command  
Technical Support Activity  
ATTN: DELSD-L  
Fort Monmouth, NJ 07703

Commander  
U.S. Army Missile Command  
ATTN: DRSMI-R  
Redstone Arsenal, AL 35809

Commander  
U.S. Army Missile Command  
ATTN: DRSMI-YDL  
Redstone Arsenal, AL 35809

Commander  
U.S. Army Natick Research  
and Development Command  
ATTN: DRXRE, D. Sieling  
Natick, MA 01762

Commander  
U.S. Army Tank Automotive Research  
and Development Command  
ATTN: DRDTA-UL  
Warren, MI 48090

Commander  
U.S. Army White Sands  
Missile Range  
ATTN: STEWS-VT  
White Sands, NM 88002

Commander  
U.S. Army Materials and  
Mechanics Research Center  
ATTN: DRXMR-ATL  
Watertown, MA 02172

Commander  
U.S. Army Research Office  
ATTN: Technical Library  
D. Squire  
F. Schmiedeshaff  
R. Ghirardelli  
M. Ciftan  
P.O. Box 12211  
Research Triangle Park, NC 27706

Director  
U.S. Army TRADOC Systems  
Analysis Activity  
ATTN: ATAA-SL  
White Sands Missile Range, NM 88002

Office of Naval Research  
ATTN: Code 473  
G. Neece  
800 N. Quincy Street  
Arlington, VA 22217

Commander  
Naval Sea Systems Command  
ATTN: J. W. Murrin, SEA-62R2  
National Center  
Bldg 2, Room 6E08  
Washington, DC 20362

Commander  
Naval Surface Weapons Center  
ATTN: Library Branch, DX-21  
Dahlgren, VA 22448

Commander  
Naval Surface Weapons Center  
ATTN: Code 240/S. J. Jacobs  
Code 730  
Silver Spring, MD 20910

Commander  
Naval Underwater Systems Center  
Energy Conversion Department  
ATTN: Code 5B331/R. S. Lazar  
Newport, RI 02840

Commander  
Naval Weapons Center  
ATTN: R. Derr  
C. Thelen  
China Lake, CA 93555

Commander  
Naval Research Laboratory  
ATTN: Code 6180  
Washington, DC 20375

Superintendent  
Naval Postgraduate School  
ATTN: Technical Library  
D. Netzer  
A. Fuhs  
Monterey, CA 93940

Commander  
Naval Ordnance Station  
ATTN: Dr. Charles Dale  
Technical Library  
Indian Head, MD 20640

AFOSR

ATTN: J. F. Masi  
B. T. Wolfson  
D. Ball  
L. Caveny  
Bolling AFB, DC 20332

AFRPL (DYSC)

ATTN: D. George  
J. N. Levine  
Edwards AFB, CA 93523

National Bureau of Standards

ATTN: J. Hastie  
T. Kashiwagi  
Washington, DC 20234

Lockheed Palo Alto Research Laboratories

ATTN: Technical Information Center  
3521 Hanover Street  
Palo Alto, CA 94304

Aerojet Solid Propulsion Co.

ATTN: P. Micheli  
Sacramento, CA 95813

ARO Incorporated

ATTN: N. Dougherty  
Arnold AFS, TN 37389

Atlantic Research Corporation

ATTN: M. K. King  
5390 Cherokee Avenue  
Alexandria, VA 22314

AVCO Corporation

AVCO Everett Research Laboratory Division  
ATTN: D. Stickler  
2385 Revere Beach Parkway  
Everett, MA 02149

Calspan Corporation

ATTN: E. B. Fisher  
A. P. Trippe  
P.O. Box 400  
Buffalo, NY 14221

Foster Miller Associates, Inc.

ATTN: A. J. Erickson  
135 Second Avenue  
Waltham, MA 02154

General Electric Company  
Armament Department  
ATTN: M. J. Bulman  
Lakeside Avenue  
Burlington, VT 05402

General Electric Company  
Flight Propulsion Division  
ATTN: Technical Library  
Cincinnati, OH 45215

Hercules Incorporated  
Alleghany Ballistic Lab  
ATTN: R. Miller  
Technical Library  
Cumberland, MD 21501

Hercules Incorporated  
Bacchus Works  
ATTN: B. Isom  
Magna, UT 84044

IITRI  
ATTN: M. J. Klein  
10 West 35th Street  
Chicago, IL 60615

Olin Corporation  
Badger Army Ammunition Plant  
ATTN: J. Ramnarace  
Baraboo, WI 53913

Olin Corporation  
New Haven Plant  
ATTN: R. L. Cook  
D. W. Riefler  
275 Winchester Avenue  
New Haven, CT 06504

Paul Gough Associates, Inc.  
ATTN: P. S. Gough  
P.O. Box 1614  
Portsmouth, NH 03801

Physics International Company  
2700 Merced Street  
Leandro, CA 94577

Pulsepower Systems, Inc.  
ATTN: L. C. Elmore  
815 American Street  
San Carlos, CA 94070

Rockwell International Corp  
Rocketdyne Division  
ATTN: C. Obert  
      J. E. Flanagan  
      A. Axeworthy  
6633 Canoga Avenue  
Canoga Park, CA 91304

Rockwell International Corp  
Rocketdyne Division  
ATTN: W. Haymes  
      Technical Library  
McGregor, TX 76657

Science Applications, Inc  
ATTN: R. B. Edelman  
Combustion Dynamics and  
  Propulsion Division  
23146 Cumorah Crest  
Woodland Hills, CA 91364

Shock Hydrodynamics, Inc  
ATTN: W. H. Anderson  
4710-16 Vineland Avenue  
N. Hollywood, CA 91602

Thiokol Corporation  
Elkton Division  
ATTN: E. Sutton  
Elkton, MD 21921

Thiokol Corporation  
Huntsville Division  
ATTN: D. Flanigan  
      R. Glick  
      Technical Library  
Huntsville, AL 35807

Thiokol Corporation  
Wasatch Division  
ATTN: J. Peterson  
      Technical Library  
P.O. Box 524  
Brigham City, UT 84302

TRW Systems Group  
ATTN: H. Korman  
One Space Park  
Redondo Beach, CA 90278

United Technologies  
Chemical Systems Division  
ATTN: R. Brown  
    Technical Library  
P.O. Box 358  
Sunnyvale, CA 94086

Universal Propulsion Co  
ATTN: H. J. McSpadden  
1800 W. Deer Valley Road  
Phoenix, AZ 85027

Battelle Memorial Institute  
ATTN: Technical Library  
    R. Bartlett  
505 King Avenue  
Columbus, OH 43201

Brigham Young University  
Dept of Chemical Engineering  
ATTN: M. W. Beckstead  
Provo, UT 84601

California Institute of Tech  
204 Karmar Lab  
Mail Stop 301-46  
ATTN: F. E. C. Culick  
1201 E. California Street  
Pasadena, CA 91125

Case Western Reserve Univ  
Division of Aerospace Sciences  
ATTN: J. Tien  
Cleveland, OH 44135

Georgia Institute of Tech  
School of Aerospace Eng  
ATTN: B. T. Zinn  
    E. Price  
    W. C. Strahle  
Atlanta, GA 30332

Institute of Gas Technology  
ATTN: D. Gidaspow  
3424 S. State Street  
Chicago, IL 60616

Johns Hopkins University/APL  
Chemical Propulsion Info Ag  
ATTN: T. Christian  
Johns Hopkins Road  
Laurel, MD 20810

Massachusetts Inst of Tech  
Dept of Mech Engineering  
ATTN: T. Toong  
Cambridge, MA 02139

Pennsylvania State University  
Applied Research Lab  
ATTN: G. M. Faeth  
P.O. Box 30  
State College, PA 16801

Pennsylvania State University  
Dept of Mechanical Engineering  
ATTN: K. Kuo  
University Park, PA 16801

Pennsylvania State University  
Dept of Material Sciences  
ATTN: H. Palmer  
University Park, PA 16801

Princeton Combustion Research  
Laboratories  
ATTN: M. Summerfield  
1041 U.S. Highway One North  
Princeton, NJ 08540

Princeton University  
Forrestal Campus  
ATTN: I. Glassman  
Technical Library  
P.O. Box 710  
Princeton, NJ 08540

Purdue University  
School of Mechanical Eng  
ATTN: J. Osborn  
S. N. B. Murthy  
TSPC Chaffee Hall  
W. Lafayette, IN 47906

Rutgers State University  
Dept of Mechanical and  
Aerospace Engineering  
ATTN: S. Temkin  
University Heights Campus  
New Brunswick, NJ 08903

SRI International  
ATTN: Technical Library  
D. Crosley  
J. Barker  
D. Golden  
333 Ravenswood Avenue  
Menlo Park, CA 94025

Stevens Institute of Tech  
Davidson Library  
ATTN: R. McAlevy, III  
Hoboken, NJ 07030

United Technology  
ATTN: Alan Ecbreth  
Research Center  
East Hartford, CT 06108

Director  
U.S. Army Materiel Systems  
Analysis Activity  
ATTN: DRXSY-MP  
Aberdeen Proving Ground, MD 21005

Commander/Director  
Chemical Systems Laboratory  
U.S. Army Armament Research and  
Development Command  
ATTN: DRDAR-CLJ-L  
DRDAR-CLB-PA  
APG, Edgewood Area, MD 21010

Director  
Ballistics Research Laboratory  
U.S. Army Armament Research and  
Development Command  
ATTN: DRDAR-TSB-S  
DRDAR-BLP, L. Watermier  
A. Barrows  
C. Nelson  
J. Vanderhoff  
J. Anderson  
Aberdeen Proving Ground, MD 21005